Journal of Materials Chemistry C

Accepted Manuscript

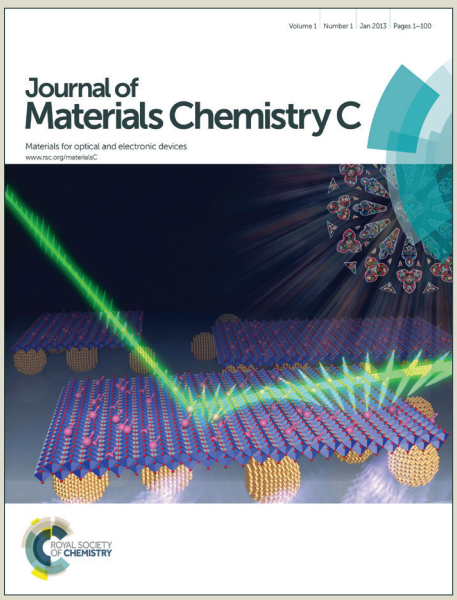

ROYAL SOCIETY OF CHEMISTRY

www.rsc.org/materialsC

Journal Name

ARTICLE

9,9-Diphenyl-thioxanthene Derivatives as Host Materials for Highly Efficient Blue Phosphorescent Organic Light-Emitting Diodes

Received 00th January 20xx,
Accepted 00th January 20xx

DOI: 10.1039/x0xx00000x
www.rsc.org/

Kunkun Liu[a], Xiang-Long Li[a], Ming Liu[a], Dongcheng Chen[a], Xinyi Cai[a], Yuan-Chun Wu[b], Chang-Cheng Lo[b], A. Lien[b], Yong Cao[a], and Shi-Jian Su[a]*

A series of 9,9-diphenyl-9*H*-thioxanthene derivatives with different sulfur atom valence states are reported as host materials in blue phosphorescent organic light-emitting diodes. Their photophysical, electrochemical and thermal properties, as well as device performance were thoroughly investigated to study their structure–property relationships, including the different carbazolyl linkage positions and sulfur atom valence states. Extremely low turn-on voltages of around 2.6 V for blue electrophosphorescence, which are already corresponding to the value of the emitted photon energy (*hv*)/electron charge (*e*), were achieved by utilizing the developed materials as the host of the blue phosphor dopant iridium(III) bis(4,6-(difluorophenyl)-pyridinato-N,$C^{2`}$)picolinate (FIrpic). Notably, a maximal power efficiency of 69.7 lm W^{-1} and extemal quantum efficiency of 29.0% were achieved for an optimal device based on m-DCz-S consisting of bivalence sulfur atom and meta-combined carbazolyl.

Introduction

Since the first report of multilayered organic light-emitting devices (OLEDs),[1] it has been extensively studied due to their practical applications as new-generation flat-panel displays and energy-saving lighting sources. With the development of phosphorescent transition metal complexes by Forrest and Ma et al.,[2,3] continuous efforts have been paid to improve the device performance of phosphorescent OLEDs (PHOLEDs). It is known that the light emission of the general fluorescent emitter originates from the radiative decay of their singlet excitons. Considering the spin selection rule, the maximum internal quantum efficiency (IQE) of the fluorescent OLEDs should be only ca. 25%. On the contrary, in the PHOLEDs, both singlet and triplet excitons can be fully utilized with a theoretical upper limit of an IQE as high as 100%. However, metal complex phosphors are necessary to be doped into an appropriate host matrix to suppress the concentration quenching and triplet–triplet annihilation. Hence development of effective host materials is of importance for efficient PHOLEDs. It is generally essential that the triplet energy (E_T) of the host is higher than that of the emitter in order to facilitate energy transfer from the host to the phosphorescent emitter and to confine the triplet excitons on the phosphors.[4,5] To meet this requirement, π-conjugation of the host materials should be limited to achieve a high enough triplet energy level. For example, molecules containing triphenylsilyl[6-8] and phosphine oxide[9] which could serve as building blocks to break the π-conjugation have been studied extensively. Moreover, it is desirable that the host material should have good carrier transport properties for balanced carrier recombination in the emitting layer and possess suitable frontier molecular orbitals to promote charge injection. Most recently, some host materials with building blocks of both electron donor and acceptor, called bipolar host materials, were developed with improved bipolarity.[10-16] So far, carbazole is considered to be a prominent hole transporting segment that can meet the above-mentioned requirements.[14,17-23] In the recent years, fluorescent materials containing sulfane or sulfone have attracted considerable attention as high efficiency fluorophors.[24-26] On the other hand, host materials containing sulfane or sulfone units for blue PHOLEDs are seldom reported. Kippelen's group[27] reported a bis-sulfone small molecule, 4,4'-bis(phenylsulfonyl)biphenyl, as a host for iridium(III) bis(4,6-(difluorophenyl)-pyridinato-N,$C^{2`}$)picolinate (FIrpic) with maximum external quantum efficiency (EQE) of 6.9% and current efficiency (CE) of 12.9 cd/A at a luminance of 100 cd/m^2. Kido's group[28] introduced a *m*-terphenyl-modified sulfone derivative, 5',5""-sulfonyldi-1,1':3',1"-terphenyl, as a host material for blue PHOLEDs with maximum EQE of 21.8% and CE of 48.6 cd/A at a luminance of 100 cd/m^2. However, there are few studies reporting host materials containing sulfane and discussing the effects of sulfur atom valence state as the host materials for blue PHOLEDs.

Here, we present a series of small molecular host materials consisting of carbazole and 9,9-diphenyl-9*H*-thioxanthene (Scheme 1). Different from fluorene, a sulfur atom is introduced to give thioxanthene with reduced π-conjugation and non-planar structure and thus higher triplet energy (E_T). In addition, sterically hindered

[a]*State Key Laboratory of Luminescent Materials and Devices and Institute of Polymer Optoelectronic Materials and Devices, South China University of Technology, Guangzhou 510640, China Fax: +86 20 87110606; Tel: +86 20 22237098; E-mail: mssjsu@scut.edu.cn*
[b]*Shenzhen China Star Optoelectronics Technology Co., Ltd., Shenzhen 518132, China*
Electronic Supplementary Information (ESI) available: Thermal analysis curves, cyclic voltammograms, and EL spectra. See DOI: 10.1039/x0xx00000x

host materials are also expected to overcome the self-quenching effect in blue PHOLEDs. As the electron-withdrawing sulfone unit generally endows the molecules improved electron affinity, bipolar characteristic is also expected for the compounds consisting of sulfone and carbazole. The thermal, electrochemical and photophysical properties of the materials have been characterized. Results indicated that these compounds exhibit good thermal stability and high E_T to be suitable as host of blue phosphorescent emitter FIrpic. Blue PHOLEDs were fabricated, and such materials possess notably variable properties when alternating the linkage position of carbazole and the valence state of sulfur atom. Extremely low turn-on voltages (V_{on}) of around 2.6 V were achieved by utilizing the developed materials as the host. Notably, the optimal device based on m-DCz-S as a host exhibited the highest CE of 65.2 cd A^{-1}, power efficiency (PE) of 69.7 lm W^{-1} and EQE of 29.0%. This is the first systematic study of the valence state of sulfur atom to develop high-triplet-energy hosts for PHOLED applications.

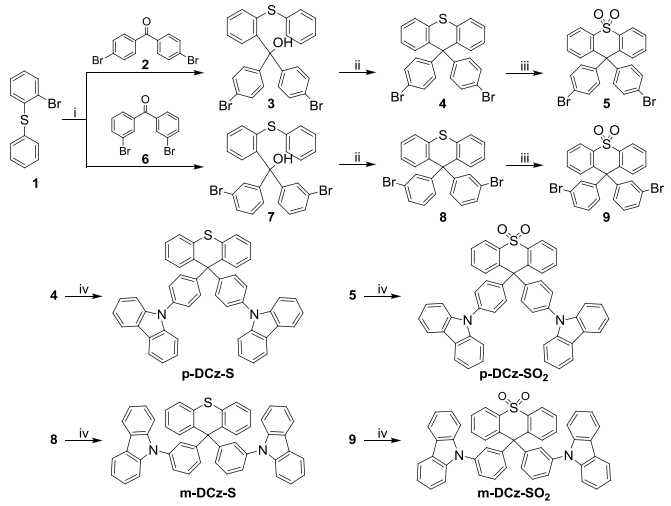

Scheme 1. Molecular structures and synthetic routes of the 9,9-diphenyl-9*H*-thioxanthene derived compounds p-DCz-S, p-DCz-SO_2, m-DCz-S, and m-DCz-SO_2. (i) n-BuLi (1 equiv), THF, −78 °C; (ii) AcOH, HCl, 80 ℃, under N_2; (iii) DCM, AcOH, H_2O_2 (5.0 equiv); (iv) carbazole, CuI, 18-crown-6, K_2CO_3, 1,3-dimethyltetrahydropyrimidin-2(1*H*)-one (DMPU), 160 ℃.

Results and discussion

The thermal stability of the target host materials was investigated by thermogravimetric analyses (TGA), and they showed high decomposition temperatures (T_d, corresponding to 5% weight loss) between 360 and 420 °C (ESI, Figure S1). According to the differential scanning calorimetry (DSC) measurements, m-DCz-S and m-DCz-SO_2 with meta-combined carbazolyl exhibit significantly high glass transition temperatures (T_g) indicating good morphological stability of their thin films in PHOLEDs. In contrast, no glass transition or other phase transition was found for p-DCz-S and p-DCz-SO_2 with para-combined carbazolyl in the same temperature range. In addition, the materials containing sulfone show higher T_d and T_g values than those containing sulfane due to the improved intermolecular interaction. The high T_d and T_g values

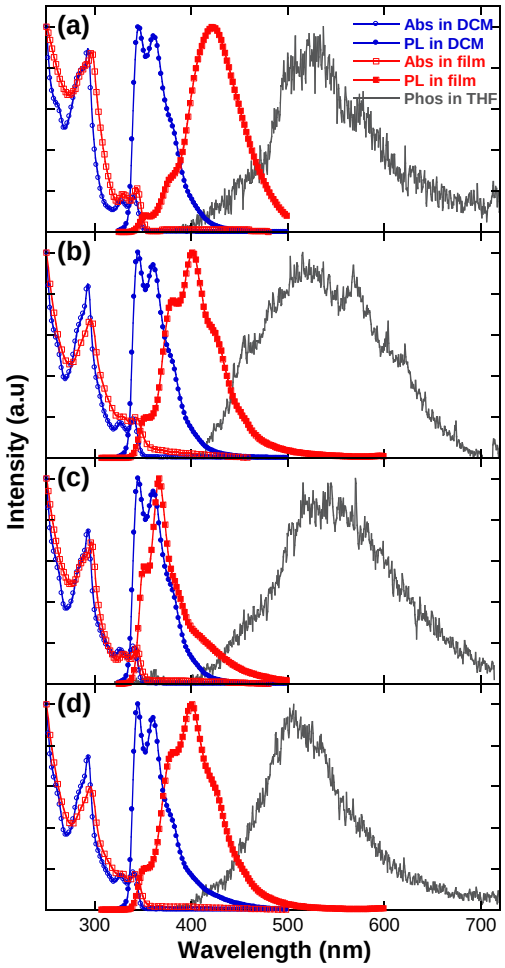

Figure 1. Normalized UV-vis absorption and photoluminescence spectra in DCM solutions (10^{-5} M) and neat thin films measured at room temperature and phosphorescence spectra measured in THF solutions (10^{-5} M) at 77 K with 1 ms delay of p-DCz-S (a), p-DCz-SO_2 (b), m-DCz-S (c), and m-DCz-SO_2 (d).

Table 1. Summary of the thermal, photophysical and electrochemical properties of p-DCz-S, p-DCz-SO_2, m-DCz-S, and m-DCz-SO_2.

compound	T_g (℃)[a]	T_d (℃)[b]	$\lambda_{PL,max}$ (nm)[c]	HOMO (eV)[d]	LUMO (eV)[e]	E_g^{opt} (eV)[f]	T_1 (eV)[g]
p-DCz-S	--	362	422	-5.26	-1.74	3.52	3.02
p-DCz-SO_2	--	404	401	-5.29	-1.80	3.49	3.01
m-DCz-S	125	385	367	-5.24	-1.72	3.52	3.03
m-DCz-SO_2	167	420	400	-5.32	-1.81	3.51	3.02

[a]Glass transition temperature (T_g) determined from DSC measurements. [b]Decomposition temperature (T_d) determined from TGA measurements (5% weight loss). [c]PL spectra measured in thin solid film. [e]HOMO energy level determined from the onset of oxidation potentials [*vs* ferrocene/ferrocenium (Fc/Fc^+)]. [e]LUMO energy level calculated from HOMO energy level and optical energy band gap. [f]Optical energy band gap as determined from the UV-vis absorption edge of the thin film. [g]Triplet energy level estimated from onset of phosphorescence spectra at 77 K.

indicate that the developed compounds are suitable for application in vacuum deposited OLEDs.

Photophysical properties of materials were measured by using ultraviolet−visible (UV−vis) and photoluminescence (PL) spectrometers. The UV-vis absorption and PL spectra of these four materials in dilute DCM solutions and in thin films were investigated systematically. As revealed in Figure 1, all the compounds exhibit sharp absorption peaks around 290 nm, which could be attributed to the π-π* transition of the carbazole moiety. From their absorption edge in film state, optical energy band gaps (E_g^{opt}) could be estimated to be 3.52, 3.49, 3.52, and 3.51 eV for p-DCz-S, p-DCz-SO_2, m-DCz-S, and m-DCz-SO_2, respectively. p-DCz-SO_2 and m-DCz-SO_2 containing sulfone show smaller E_g^{opt}s than p-DCz-S and m-DCz-S containing sulfane, which could be attributed to the stronger electron affinity of sulfone and thus stronger intramolecular charge transfer (ICT).

The developed materials show similar PL spectra in ultraviolet region in dilute DCM solutions. However, they are quite different in thin films. Among them, p-DCz-S with para-combined carbazoly shows the largest bathochromic emission shift from 341 nm in DCM solution to 423 nm in thin film, which may be attributed to the strongest molecular packing. And such state may induce potential quenching sites.[9,29] In contrast, m-DCz-S with meta-combined carbazoly shows quite small bathochromic shift. In comparison, the p-DCz-SO_2 and m-DCz-SO_2 films show similar bathochromic emission shift which is between those of the p-DCz-S and m-DCz-S films. It may be affected by the different sulfur atom valence states.

From the phosphorescence spectra measured in frozen THF at 77 K, triplet energy levels of p-DCz-S, p-DCz-SO_2, m-DCz-S, and m-DCz-SO_2 were estimated to be 3.02, 3.01, 3.03, and 3.02 eV, respectively. They are much higher than the triplet energy of the general blue phosphor FIrpic due to their reduced π-conjugation and non-planar structure. To further verify their triplet exciton confinement ability, FIrpic was co-deposited with the host materials for transient PL decay measurements by time-correlated single photon counting method detected at 472 nm according to the emission peak of FIrpic under the excitation of a nanosecond lamp (λ=290 nm).

As shown in Figure 2, it can be clearly seen that all the co-deposited films with FIrpic exhibit clearly monoexponential decay curves with relatively long lifetimes between 1.1 and 1.3 μs (Table 2). In addition, the co-deposited films of p-DCz-SO_2:FIrpic, m-DCz-S:FIrpic, and m-DCz-SO_2:FIrpic exhibit very high PL quantum yields (η_{PL}) of above 89%, which can be attributed to efficient energy transfer from the host to the guest and good confinement of triplet energy on the FIrpic molecules. In contrast, the co-deposited film of p-DCz-S:FIrpic exhibits a much lower η_{PL} of 57.6%, and it may be attributed to the easier molecular packing of p-DCz-S to be as potential quenching sites. Among these co-deposited films, m-DCz-S:FIrpic exhibits the largest radiative rate constant (k_r) of 8.03×10^5 s^{-1} and the smallest nonradiative rate constant (k_{nr}) of 0.23×10^5 s^{-1}. The monoexponential decay behavior and the highest PL quantum yield for the film of m-DCz-S:FIrpic prove that the triplet energy transfer from FIrpic to m-DCz-S is successfully suppressed and the energy is well-confined on the phosphor molecules.

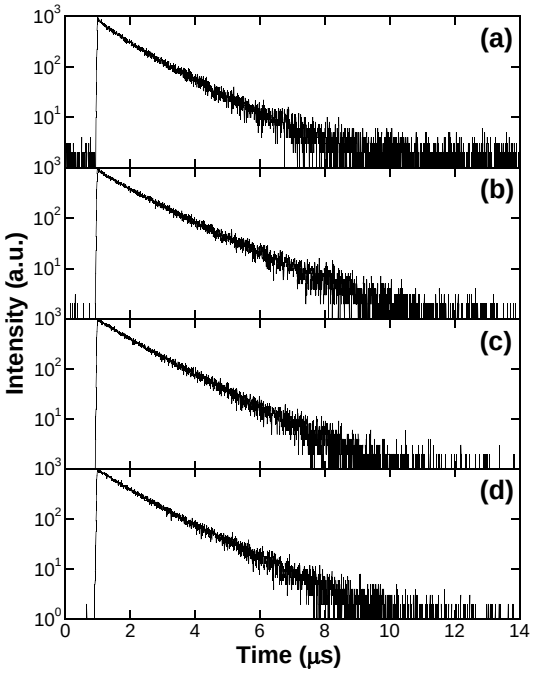

Figure 2. Transient PL decay curves of the co-deposited films of p-DCz-S: FIrpic (a), p-DCz-SO_2:FIrpic (b), m-DCz-S:FIrpic (c), and m-DCz-SO_2: FIrpic (d) in a doping concentration of 12 wt%.

Table 2. Summary of phosphorescence lifetime (τ), photoluminescence quantum yield (η_{PL}), radiative and nonradiative rate constants (k_r and k_{nr}) of FIrpic co-deposited with p-DCz-S, p-DCz-SO_2, m-DCz-S, and m-DCz-SO_2.

host	τ (μs)	η_{PL}(%)	k_r ($\times10^5$ s^{-1})	k_{nr} ($\times10^5$ s^{-1})
p-DCz-S	1.11	57.6	5.19	3.82
p-DCz-SO_2	1.30	89.3	6.87	0.82
m-DCz-S	1.21	97.2	8.03	0.23
m-DCz-SO_2	1.21	90.2	7.45	0.81

The electrochemical behaviors of the materials were investigated by cyclic voltammetry (CV) (Figure S2). Their highest occupied molecular orbital (HOMO) energy levels were estimated to be -5.24 – -5.32 eV according to the oxidation potentials and the ionization potential (4.8 eV) of ferrocene/ferrocenium (Fc/Fc^+). The lowest unoccupied molecular orbital (LUMO) energy levels estimated from HOMO energy levels and E_g^{opt}s were -1.72 to -1.81 eV.

DFT calculations were also performed to gain further insight into the electronic states of these materials by using Gaussian 09W program.[31] As shown in Figure 3, HOMOs of all the compounds mainly locate at the peripheral carbazole moieties, while their LUMOs mainly locate at the central thioxanthene or thioxanthene-10,10-dioxide unit. As a result, lower-lying LUMO energy levels are obtained for the compounds containing sulfone than those containing sulfane. In comparison, their HOMO energy levels are slightly influenced by the change of sulfur atom valence state. The calculated

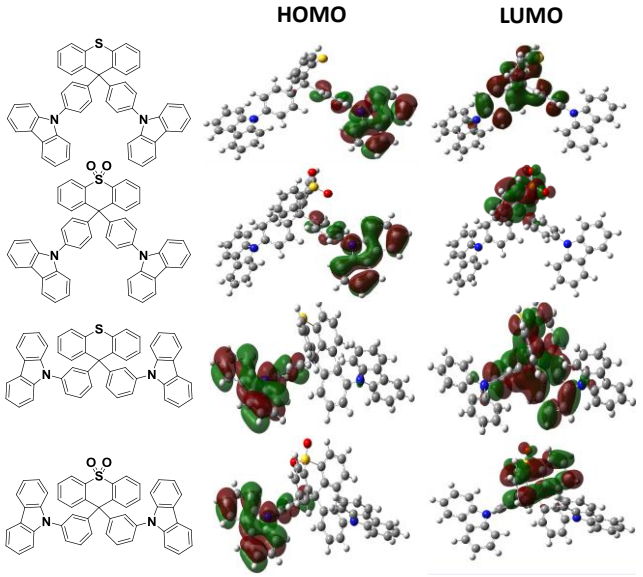

Figure 3. Calculated spatial distributions of HOMOs and LUMOs of p-DCz-S, p-DCz-SO_2, m-DCz-S, and m-DCz-SO_2.

Table 3. Summary of the theoretical calculations of p-DCz-S, p-DCz-SO_2, m-DCz-S, and m-DCz-SO_2 (DFT, B3LYP/6-31G (d) and TD-DFT, B3LYP/ 6-31G (d), Gaussian 09W_B01).

compound	HOMO (eV)	LUMO (eV)	S_1 (eV)	T_1 (eV)
p-DCz-S	-5.33	-0.90	3.93	3.18
p-DCz-SO_2	-5.32	-1.47	3.49	3.18
m-DCz-S	-5.33	-0.91	3.97	3.18
m-DCz-SO_2	-5.35	-1.44	3.48	3.18

HOMO energy levels of these compounds are around 5.33 eV, which show good agreement with the experimental results. Vertical transition energy of singlet and triplet excited state energy are also calculated, as shown in Table 3. T_1 levels of all the compounds were calculated to be 3.18 eV, and the their similar high triplet energies might be attributed to the reduced π-conjugation and non-planar structure.

To investigate the performance of these materials as host of blue phosphor, PHOLEDs were fabricated by doping FIrpic into the developed materials as emission layer (EML) in a configuration of ITO (95 nm)/ HATCN (5 nm)/ NPB (30 nm)/ TAPC (10 nm)/ Host: 12wt% FIrpic (10 nm)/ TmPyPB (40 nm)/ LiF (1 nm)/ Al (90 nm), where ITO (indium tin oxide) and LiF/Al are the anode and the cathode, respectively; NPB (4,4'-bis[N-(1-naphthyl)-N-phenylamino]biphenyl) is the hole-transporting layer (HTL); A thin TAPC (1,1-bis(4-(N,N-di(p-tolyl)-amino)-phenyl)cyclohexane) layer is inserted between the HTL and EML in order to confine triplet excitons more effectively in the EML; and TmPyPB serves as the electron-transporting layer (ETL) and the hole-blocking layer. Considering the huge hole injection barrier between ITO (-4.8 eV) and NPB (-5.4 eV), HATCN (dipyrazino(2,3-f:2',3'-h)-quinoxaline -2,3,6,7,10,11-hexacarbonitrile) is used as the anode buffer layer to encourage the hole injection into the HTL. Electroluminescence (EL) spectra of the devices are depicted in Figure S2. All the EL spectra show similar spectral characteristics with a λ_{EL} of 472 nm and CIE coordinates of (0.16, 0.33), corresponding to the emission of FIrpic.

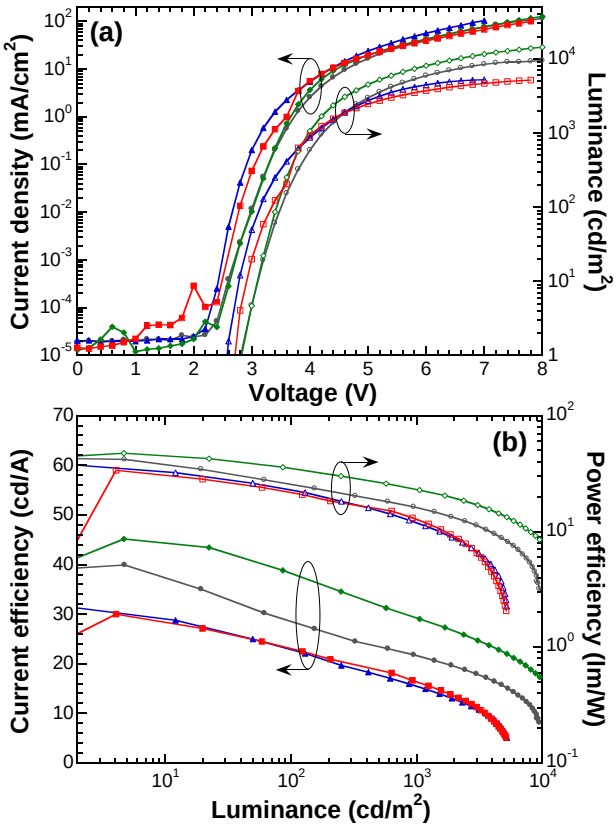

Figure 4. Current density–voltage–luminance (J–V–L) (a) and current efficiency (CE)–luminance–power efficiency (PE) (b) characteristics of the PHOLEDs in a structure of ITO (95 nm)/ HATCN (5 nm)/ NPB (30 nm)/ TAPC (10 nm)/ Host: 12wt% FIrpic (10 nm)/ TmPyPB (40 nm)/ LiF (1 nm)/Al (90 nm). Host: p-DCz-S (○●), p-DCz-SO_2 (△▲), m-DCz-S (◇◆), and m-DCz-SO_2 (□■).

Moreover, no additional emission coming from the host materials was observed, indicating efficient energy transfer from the host to the dopant.

As shown in Figure 4, it can be observed that the devices based on these hosts exhibit extremely low turn-on voltages (V_{on}) (at the luminance of 1 cd m^{-2}) of 2.6-2.8 V, which are readily comparable to the value of the photon energy ($h\nu$ = 2.63 eV, corresponding to the peak emission wavelength of 472 nm) divided by the electron charge (e). Extremely low V_{on} of 2.6 V is realized for the device based on p-DCz-SO_2, which is among the lowest ones for the FIrpic-based devices with single host.[10,31,32] Note that FIrpic is a well-known electron-transport triplet emitter and the doping concentration of FIrpic is relatively high (12 wt%). Considering the lower-lying LUMO energy level of TmPyPB, electrons may be partly injected into the EML through the FIrpic molecules. The low turn-on voltages could be ascribed to the effective hole injection due to suitable HOMO energy levels of the developed host materials. Among the fabricated blue PHOLEDs, the highest efficiency was achieved for the device based on m-DCz-S, which gave a maximum CE of 45.1 cd A^{-1} and a maximum PE of 46.1 lm W^{-1}, while lower values of 39.9 cd A^{-1} and 39.9 lm W^{-1} were obtained for the device based on p-DCz-S. However, the devices based on p-DCz-SO_2 and m-DCz-SO_2 containing sulfone show further poorer performance compared with those based on m-DCz-S and p-DCz-S containing

Table 4. Summary of the performance of the PHOLEDs based on the developed host materials.

Host	V_{on}	maximum efficiency			at 100 cd/m^2				at 1000 cd/m^2			
	(V)	CE (cd/A)	PE (lm/W)	EQE (%)	V (V)	CE (cd/A)	PE (lm/W)	EQE (%)	V (V)	CE (cd/A)	PE (lm/W)	EQE (%)
p-DCz-S[a]	2.8	39.9	39.9	18.5	3.5	28.6	25.8	13.3	4.2	21.8	16.3	10.1
p-DCz-SO_2[a]	2.6	31.5	32.3	15.6	3.2	22.1	21.67	10.9	4.0	15.4	11.9	7.6
m-DCz-S[a]	2.8	45.1	47.3	20.8	3.4	38.1	35.3	17.8	4.0	29.0	22.8	13.4
m-DCz-SO_2[a]	2.8	30.0	33.7	13.4	3.4	23.1	21.0	10.3	4.0	16.6	13.1	7.4
m-DCz-S[b]	2.8	65.2	69.7	29.0	3.4	50.1	47.1	22.4	4.0	37.7	29.6	16.7

[a]Device structure: ITO (95 nm)/ HATCN (5 nm)/ NPB (30 nm)/ TAPC (10 nm)/ Host: 12wt% FIrpic (10 nm)/ TmPyPB (40 nm)/ LiF (1 nm)/Al (90 nm).
[b]Device structure: ITO (95 nm) / TAPC (40 nm)/ Host: 12wt% FIrpic (10 nm)/ TmPyPB (40 nm)/ LiF (1 nm)/Al (90 nm).

sulfane, which only show a maximum CE of approximately 30 cd A^{-1} and a maximum PE of about 33 lm W^{-1}.

Since the charge carriers are recombined in the EML in an OLED, balanced carrier injection and transport into the EML is a prerequisite for improved device performance. As thus, balanced hole and electron mobility is extremely of importance for a host material. To study bipolar properties and different performance of these host materials, hole-only and electron-only devices were also fabricated. The configuration of the hole-only devices (HOD) is ITO (95 nm)/ HATCN (5 nm)/ NPB (30 nm)/ TAPC (10 nm)/ Host (10 nm)/ TAPC (40 nm)/ Al (90 nm), and the electron-only devices (EOD) have a structure of ITO (95 nm)/ TmPyPB (40 nm)/ Host (10 nm)/ TmPyPB (40 nm)/ LiF (1 nm)/ Al (90 nm). TAPC (LUMO: -2.0 eV) on the cathode side of the HODs and TmPyPB (HOMO: -6.45 eV) on the anode side of the EODs are utilized to block the electron-injection from Al (work-function: 4.3 eV, corresponding to a large energy barrier of 2.3 eV) and the hole-injection from ITO (work-function: 4.8 eV, corresponding to a large energy barrier of 1.65 eV), respectively. As shown in Figure 5, m-DCz-S and p-DCz-S show better hole transport ability than p-DCz-SO_2 and m-DCz-SO_2, indicating the sulfone unit may lead to decreased hole transport. On the other hand, p-DCz-SO_2 and m-DCz-SO_2 show higher electron transport ability due to the electron-withdrawing sulfone. As aforementioned, FIrpic is an electron-transport triplet emitter. The relatively higher electron transport ability may induce an electron dominant current and thus reduced carrier balance and lower device performance. It is of interest m-DCz-S still show good electron transport ability and the highest hole transport ability, which suggests that m-DCz-S may possess the best balanced hole/electron

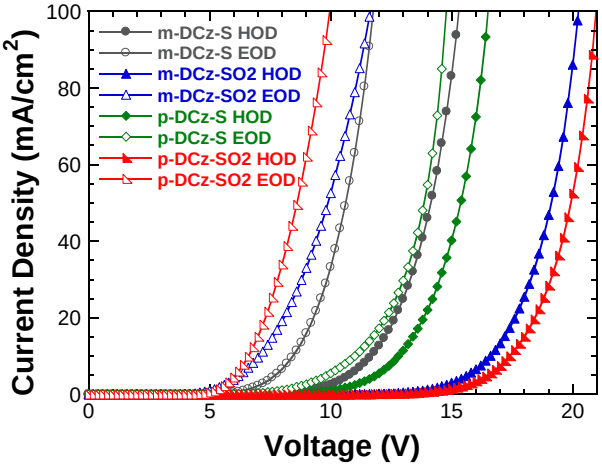

Figure 5. Current density versus voltage characteristics for the hole-only devices (HOD) and electron-only devices (EOD).

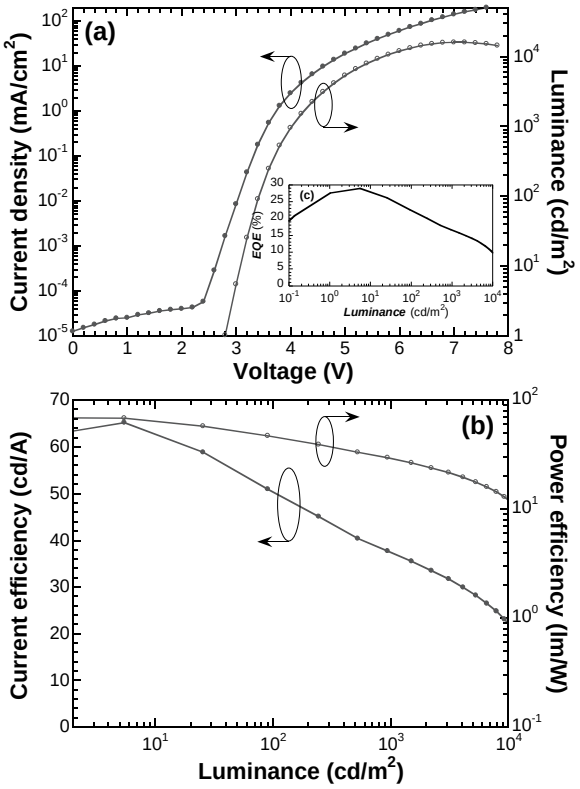

Figure 6. Current density–voltage–luminance (J–V–L) (a), current efficiency (CE)–luminance–power efficiency (PE) (b), and external quantum efficiency (EQE)–luminance (c, inset) characteristics of the device based on m-DCz-S in a structure of ITO (95 nm)/ TAPC (40 nm)/ m-DCz-S: 12 wt% FIrpic (10 nm)/ TmPyPB (40 nm)/ LiF (1 nm)/ Al (90 nm).

injection and transport properties among these host materials. Aside from the bipolar charge transport capability and good carrier balance, the highest PL quantum yield (97.2%) of the FIrpic doped with m-DCz-S is also of benefit to the remarkable performance of the device based on m-DCz-S.

Whereas, according to the equation: $EQE_{max} = \eta_{op} \times \eta_{PL} \times \eta_r \times \gamma$, where η_{op} is the optical out-coupling factor, η_r is the ratio of radiative excitons, and γ is the carrier balance factor, we can predict that the theoretical EQE_{max} for the device based on m-DCz-S should reach a value of 29.2%, given that η_{op} is 30% and γ is 1. It is deduced that the carrier balance in the previous device based on m-DCz-S was still imperfect, leading to a lower EQE than that of the theoretically optimal device. Thus, we further optimized the device structure in a configuration of ITO (95 nm)/ TAPC (40 nm)/ m-DCz-S: 12 wt% FIrpic (10 nm)/ TmPyPB (40 nm)/ LiF (1 nm)/ Al (90 nm). Accordingly, as shown in Figure 6, the optimized device exhibits a

turn-on voltage of 2.8 V, and the luminance reaches 100 and 1000 cd m^{-2} at 3.4 and 4.0 V, respectively. In addition, a maximum EQE of 29.0% was obtained for the optimized device, which is in good agreement with the theoretical maxima, indicating a well-balanced carrier was achieved for the optimized device. Moreover, the hitherto highest PE value of 69.7 lm W^{-1} was achieved at low luminance (Table S1),[29,32-36] and it maintains as high as 47.1 and 29.6 lm W^{-1} at the brightness of 100 and 1000 cd m^{-2}, respectively.

Conclusions

In summary, a series of 9,9-diphenyl-9*H*-thioxanthene derivatives were developed as the host materials for blue PHOLEDs. Their photophysical, electrochemical, and thermal properties have been studied systematically. With the different carbazolyl linkage positions and sulfur atom valence states, the materials show tremendous difference in device performance. Extremely low turn-on voltages of around 2.6 V were achieved by the developed materials. In addition, an enhanced device performance was achieved by m-DCz-S consisting of sulfane and meta-combined carbazolyl with maximum EQE of 29.0%, CE of 65.2 cd A^{-1}, and PE of 69.7 lm W^{-1}, indicating that m-DCz-S is a potential host material for blue PHOLEDs. This is the first systematic study of the effect of sulfur atom valence state to develop high-triplet-energy host materials for PHOLED applications, and the present findings give a new route to further improve the performance of PHOLEDs through lowering the operating voltage.

Experimental

General. All the developed host materials were purified by silica gel chromatography and then repeated thermal gradient vacuum sublimation before characterization and device fabrication. ^{1}H NMR spectra were recorded on a Bruker NMR spectrometer operating at 600 or 500 MHz, and ^{13}C NMR spectra were recorded at 150 MHz. TGA was undertaken on a Netzsch TG 209 under N_2 flow at a heating rate of 10 ℃ min^{-1}. DSC measurements were performed on a Netzsch DSC 209 under N_2 flow at a heating and cooling rate of 10 ℃ min^{-1}. UV-vis absorption spectra were measured on a HP 8453 spectrophotometer. PL spectra were recorded on a Horiba Fluoromax-4 spectrofluorometer. CV was performed on a CHI600D electrochemical workstation with a platinum working electrode and a platinum wire counter electrode at a scanning rate of 100 mV s^{-1} against a Ag/Ag^+ (0.1 M of $AgNO_3$ in acetonitrile) reference electrode with a nitrogen-saturated anhydrous acetonitrile and dichloromethane solution of 0.1 mol L^{-1} tetrabutylammonium hexafluorophosphate. PL quantum yields of the films were measured under air condition by using an integrating sphere on a HAMAMATSU absolute PL quantum yield spectrometer C11347. Transient PL spectra were measured with an Edinburgh FL920 fluorescence spectrophotometer. PL decays and the corresponding simultaneous PL spectra of the phosphorescent emitter-doped films were recorded at room temperature. The thin solid films used for absorption and PL spectral measurements were vacuum vapor deposited on quartz substrates.

Materials. All solvents and reagents were used as received from commercial suppliers without further purification. 2-Bromophenyl-phenyl-sulfane (**1**) was synthesized according to literature.[30] Synthetic routes of the object compounds are outlined in Scheme 1.

*9,9-bis(4-bromophenyl)-9H-thioxanthene (**4**).* **1** (2.65 g, 10 mmol) was dissolved in dry tetrahydrofuran (THF) and degassed for 15 min. The resulting mixture was cooled to −78 °C under nitrogen, and n-butyllithium (1.6 M in hexanes) (7 mL, 11 mmol) was added in a dropwise manner. The resulting mixture was stirred at −78 °C for 1 h, and then bis(4-bromo-phenyl) ketone (**2**) (3.40 g, 10 mmol) in dry THF was added in one portion. After stirred overnight, the resulting mixture was quenched with deionized water and extracted with dichloromethane (DCM) for three times. The combined organic layer was then washed with deionized water. The solution was dried over anhydrous $MgSO_4$ and filtered. The solvent was removed by distillation under reduced pressure. Bis(4-bromophenyl)(2-(phenyl-thio) phenyl)methanol (**3**) was purified by column chromatography and used for the next step directly. A mixture of **3**, 50 ml acetic acid (AcOH), and 3 ml chloride acid was stirred under argon at 80 ℃ for 3h. The reaction mixture was extracted with DCM and further purified by column chromatography to give a white solid (3.04 g, total yield 60%). ^{1}H NMR (500 MHz, $CDCl_3$, δ, ppm): 7.45 (dd, *J* = 7.7, 0.9 Hz, 2H), 7.39-7.34 (m, 4H), 7.29-7.24 (m, 2H), 7.22-7.13 (m, 2H), 6.90 (d, *J* = 7.9 Hz, 2H), 6.68-6.62 (m, 4H). MS (APCI, m/z): $[M]^+$ calcd for $C_{25}H_{16}Br_2S$, 507.93; found: 508.9362.

*9,9-bis(4-bromophenyl)-9H-thioxanthene 10,10-dioxide (**5**).* A mixture of **4** (3.04 g, 6 mmol), 10 ml DCM, 30 ml AcOH, 6 ml H_2O_2 (60 mmol, 10 equ) was stirred under atmosphere at 80 ℃ for 24h. The reaction mixture was extracted with DCM and further purified by column chromatography to give a white solid (2.58 g, yield 88%). ^{1}H NMR (500 MHz, $CDCl_3$, δ, ppm): 8.22 (dd, *J* = 7.6, 0.8 Hz, 2H), 7.58 (t, *J* = 7.6 Hz, 2H), 7.51 (td, *J* = 7.8, 1.3 Hz, 2H), 7.40 (d, *J* = 8.6 Hz, 4H), 6.99 (d, *J* = 7.9 Hz, 2H), 6.68 (d, *J* = 8.6 Hz, 4H). MS (APCI, m/z): $[M]^+$ calcd for $C_{25}H_{16}Br_2O_2S$, 539.92; found: 540.9292.

*9,9-bis(3-bromophenyl)-9H-thioxanthene (**8**).* **8** was synthesized in a similar manner of **4** with bis(3-bromophenyl)ketone (**6**) in place of **2** to give a white solid (3.40 g, yield 60%). ^{1}H NMR (500 MHz, $CDCl_3$, δ, ppm): 7.46 (dd, *J* = 7.7, 1.2 Hz, 2H), 7.44 – 7.40 (m, 2H), 7.30-7.25 (m, 2H), 7.20 (td, *J* = 7.8, 1.3 Hz, 2H), 7.12 (t, *J* = 7.9 Hz, 2H), 6.92-6.87 (m, 4H), 6.71 (dd, *J* = 7.9, 0.7 Hz, 2H). MS (APCI, m/z): $[M]^+$ calcd for $C_{25}H_{16}Br_2S$, 507.93; found: 508.9362.

*9,9-bis(3-bromophenyl)-9H-thioxanthene 10,10-dioxide (**9**).* The synthetic process was performed as **5** with **8** in place of **4** to give a white solid (2.58 g, yield 81%). ^{1}H NMR (500 MHz, $CDCl_3$, δ, ppm): 8.23 (dd, *J* = 7.7, 1.2 Hz, 1H), 7.59 (td, *J* = 7.6, 0.8 Hz, 1H), 7.54 (td, *J* = 7.7, 1.4 Hz, 1H), 7.45 (dd, *J* = 8.0, 0.7 Hz, 1H), 7.16 (t, *J* = 8.0 Hz, 1H), 7.00 (d, *J* = 7.8 Hz, 1H), 6.73 (dd, *J* = 8.0, 0.8 Hz, 1H). MS (APCI, m/z): $[M]^+$ calcd for $C_{25}H_{16}Br_2O_2S$, 539.92; found: 540.9292.

9,9'-((9H-thioxanthene-9,9-diyl)bis(4,1-phenylene))bis(9H-carbazole) (p-DCz-S). **5** (0.608 g, 1.2 mmol), carbazole (0.44 g, 2.64 mmol), CuI (0.24 g), 18-crown-6 (0.33 g), K_2CO_3 (0.36 g), and 1,3-dimethyltetrahydropyrimidin-2(1*H*)-one (DMPU) (8 ml) were added to a 20 ml three-necked round-bottomed flask. The mixture was

stirred and heated at 160 ℃ for 24 h under a nitrogen atmosphere and then cooled to room temperature. The resulting mixture was extracted with DCM and dried over Na_2SO_4, and then concentrated under vacuum. The residue was purified by column chromatography on silica gel to give a white solid (0.57 g, yield 71%). ^{1}H NMR (500 MHz, $CDCl_3$, δ, ppm): 8.16 (d, *J* = 7.7 Hz, 4H), 7.57 (dd, *J* = 7.4, 1.5 Hz, 2H), 7.55-7.50 (m, 8H), 7.47-7.41 (m, 4H), 7.34 (dtd, *J* = 14.7, 7.5, 1.0 Hz, 8H), 7.18 (dd, *J* = 7.7, 1.4 Hz, 2H), 7.13 (d, *J* = 8.6 Hz, 4H).^{13}C NMR (126 MHz, $CDCl_3$, δ, ppm): 142.94, 141.60, 140.65, 136.44, 133.91, 132.11, 130.96, 127.15, 127.07, 126.10, 125.94, 125.91, 123.44, 120.33, 120.03, 109.84, 61.44. MS (MALDI-TOF): m/z calcd for $C_{49}H_{32}N_2S$: 680.2; found: 679.199.

9,9-bis(4-(9H-carbazol-9-yl)phenyl)-9H-thioxanthene 10,10-dioxide (p-DCz-SO$_2$). p-DCz-SO_2 (0.59 g, yield 70%) was synthesized as a white solid in a similar manner of p-DCz-S with **5** instead of **4**. ^{1}H NMR (600 MHz, $CDCl_3$, δ, ppm): 8.34 (dd, *J* = 5.5, 3.6 Hz, 1H), 8.15 (d, *J* = 7.7 Hz, 2H), 7.66 (dt, *J* = 7.0, 3.5 Hz, 2H), 7.57 (d, *J* = 8.4 Hz, 2H), 7.50 (d, *J* = 8.2 Hz, 2H), 7.43 (t, *J* = 7.7 Hz, 2H), 7.33-7.25 (m, 3H), 7.18 (d, *J* = 8.4 Hz, 2H). ^{13}C NMR (126 MHz, $CDCl_3$, δ, ppm): 144.89, 143.08, 140.52, 137.58, 137.05, 132.19, 131.75, 131.69, 128.51, 126.53, 125.98, 124.50, 123.50, 120.35, 120.17, 109.77, 58.84. MS (MALDI-TOF): m/z calcd for $C_{49}H_{32}N_2O_2S$: 712.22; found: 712.226.

9,9'-((9H-thioxanthene-9,9-diyl)bis(3,1-phenylene))bis(9H-carbazole) (m-DCz-S). m-DCz-S (0.58 g, yield 70%) was synthesized as a white solid in a similar manner of p-DCz-S with **8** instead of **4**. ^{1}H NMR (500 MHz, $CDCl_3$, δ, ppm): 8.11-8.02 (m, 4H), 7.53 (dd, *J* = 7.7, 1.2 Hz, 2H), 7.51-7.44 (m, 4H), 7.32-7.16 (m, 18H), 7.14 (dd, *J* = 7.9, 1.1 Hz, 2H), 6.96 (dt, *J* = 7.2, 1.7 Hz, 2H). ^{13}C NMR (126 MHz, $CDCl_3$, δ, ppm): 145.62, 141.34, 140.31, 137.35, 133.75, 130.85, 129.22, 129.13, 129.10, 127.20, 126.93, 126.05, 125.87, 125.01, 123.36, 120.17, 119.96, 109.69, 61.71. MS (MALDI-TOF): m/z calcd for $C_{49}H_{32}N_2S$: 680.2; found: 679.199.

9,9-bis(3-(9H-carbazol-9-yl)phenyl)-9H-thioxanthene 10,10-dioxide (m-DCz-SO$_2$). m-DCz-SO_2 (0.60 g, yield 72%) was synthesized as a white solid in a similar manner of p-DCz-S with **9** instead of **5**. ^{1}H NMR (600 MHz, $CDCl_3$, δ, ppm): 8.32 (d, *J* = 7.6 Hz, 1H), 8.10 (d, *J* = 8.6 Hz, 2H), 7.67-7.52 (m, 4H), 7.26 (t, *J* = 10.3 Hz, 7H), 7.16 (s, 1H), 7.04 (dd, *J* = 7.5, 5.0 Hz, 1H).^{13}C NMR (126 MHz, $CDCl_3$, δ, ppm): 145.89, 144.57, 140.32 , 137.83, 137.65, 132.14, 131.53, 129.70, 128.80, 128.69, 128.54, 125.97, 125.85, 124.48, 123.38, 120.21, 120.09, 109.59, 59.10. MS (MALDI-TOF): m/z calcd for $C_{49}H_{32}N_2O_2S$: 712.22; found: 712.226.

Theoretical Calculations. Theoretical calculation of the compounds was carried out by using Gaussian 09_B01 package. Density functional theory (DFT) calculation in B3LYP/6-31G(d) basis set was performed to determine the ground state structure in gas phase. Theoretical prediction for energy levels of the compounds was acquired based on the optimized structure. B3LYP/6-31G(d) functional was utilized to gain insight into the character of the excited singlet states (S_1) and triplet states (T_1) by using the optimized structure mentioned above.

Device Fabrication and Characterization. Phosphorescent OLEDs were grown on glass substrates pre-coated with a 95-nm-thin layer of indium tin oxide (ITO) with a sheet resistance of 10 Ω per square. The substrates were thoroughly cleaned in ultrasonic bath of acetone, isopropyl alcohol, detergent, deionized water, and isopropyl alcohol and treated with O_2 plasma for 20 min in sequence. Organic layers were deposited onto the ITO-coated substrates by high-vacuum ($<5\times10^{-4}$ Pa) thermal evaporation. Cathodes consisting of a 1-nm-thin layer of LiF followed by a 90-nm-thin layer of Al, were patterned using a shadow mask with an array of 3 mm×3 mm openings. Deposition rates are 1~2 Å/s for organic materials, 0.1 Å/s for LiF, and 6 Å/s for Al, respectively. EL spectra were recorded by an optical analyzer, Photo Research PR705. The current density and luminance versus driving voltage characteristics were acquired by Keithley 2420 and Konica Minolta chromameter CS-200, respectively. EQE was calculated from the luminance, current density, and EL spectrum, assuming a Lambertian distribution.

Acknowledgements

The authors greatly appreciate the financial support from the Ministry of Science and Technology (2015CB655003 and 2014DFA52030), the National Natural Science Foundation of China (91233116 and 51073057), the Ministry of Education (NCET-11-0159), and the Guangdong Natural Science Foundation (S2012030006232). The authors are grateful to Shitong Zhang for his help in low temperature phosphorescence measurements.

Notes and references

1. C. W. Tang, S. Vanslyke, *Appl. Phys. Lett.*, 1987, **51**, 913.
2. M. A. Baldo, D. F. O'Brien, Y. You, A. Shoustikov, S. Sibley, M. E. Thompson, S. R. Forrest, *Nature*, 1998, **395**, 151.
3. Y. G. Ma, H. Y. Zhang, J. C. Shen, C. M. Che, *Synthetic Met*, 1998, **94**, 245.
4. R. J. Holmes, S. R. Forrest, Y. J. Tung, R. C. Kwong, J. J. Brown, S. Garon, M. E. Thompson, *Appl. Phys. Lett.*, 2003, **82**, 2422.
5. S. Tokito, T. Iijima, Y. Suzuri, H. Kita, T. Tsuzuki, F. Sato, *Appl. Phys. Lett.*, 2003, **83**, 569.
6. S. J. Yeh, M. F. Wu, C. T. Chen, Y. H. Song, Y. Chi, M. H. Ho, S. F. Hsu, C. H. Chen, *Adv. Mater.*, 2005, **17**, 285.
7. M. H. Tsai, H. W. Lin, H. C. Su, T. H. Ke, C. C. Wu, F. C. Fang, Y. L. Liao, K. T. Wong, C. I. Wu, *Adv. Mater.*, 2006, **18**, 1216.
8. P. I. Shih, C. H. Chien, C. Y. Chuang, C. F. Shu, C. H. Yang, J. H. Chen, Y. Chi, *J. Mater. Chem.*, 2007, **17**, 1692.
9. L. S. Sapochak, A. B. Padmaperuma, X. Y. Cai, J. L. Male, P. E. Burrows, *J. Phys. Chem. C*, 2008, **112**, 7989.
10. S. J. Su, H. Sasabe, T. Takeda, J. Kido, *Chem. Mater.*, 2008, **20**, 1691.
11. S. J. Su, C. Cai, J. Kido, *Chem. Mater.*, 2011, **23**, 274.
12. S. J. Su, C. Cai, J. Kido, *J. Mater. Chem.*, 2012, **22**, 3447.
13. S. J. Su, C. Cai, J. Takamatsu, J. Kido, *Org. Electron*., 2012, **13**, 1937.
14. K. Brunner, A. van Dijken, H. Borner, J. J. Bastiaansen, N. M. Kiggen, B. M. Langeveld, *J. Am. Chem. Soc.*, 2004, **126**, 6035.
15. Y. T. Tao, Q. Wang, C. L. Yang, Q. Wang, Z. Q. Zhang, T. T. Zou, J. G. Qin, D. G. Ma, *Angew. Chem. Int. Edit*, 2008, **47**, 8104.
16. F. M. Hsu, C. H. Chien, P. I. Shih, C. F. Shu, *Chem. Mater.*, 2009, **21**, 1017.
17. P. I. Shih, C. L. Chiang, A. K. Dixit, C. K. Chen, M. C. Yuan, R. Y. Lee, C. T. Chen, E. W. G. Diau, C. F. Shu, *Org. Lett.*, 2006, **8**, 2799.

18. M. H. Tsai, Y. H. Hong, C. H. Chang, H. C. Su, C. C. Wu, A. Matoliukstyte, J. Simokaitiene, S. Grigalevicius, J. V. Grazulevicius, C. P. Hsu, *Adv. Mater.*, 2007, **19**, 862.
19. H. Fukagawa, K. Watanabe, T. Tsuzuki, S. Tokito, *Appl. Phys. Lett.*, 2008, **93**, 133312.
20. S. O. Jeon, K. S. Yook, C. W. Joo, J. Y. Lee, *Adv. Funct. Mater.*, 2009, **19**, 3644.
21. S. O. Jeon, K. S. Yook, C. W. Joo, J. Y. Lee, *Adv. Mater.*, 2010, **22**, 1872.
22. H. H. Chou, C. H. Cheng, *Adv. Mater.*, 2010, **22**, 2468.
23. D. C. Chen, S. J. Su, Y. Cao, *J. Mater. Chem. C*, 2014, **2**, 9565.
24. Q. S. Zhang, J. Li, K. Shizu, S. P. Huang, S. Hirata, H. Miyazaki, C. Adachi, *J. Am. Chem. Soc.*, 2012, **134**, 14706.
25. C. J. Zheng, J. Wang, J. Ye, M. F. Lo, X. K. Liu, M. K. Fung, X. H. Zhang, C. S. Lee, *Adv. Mater.*, 2013, **25**, 2205.
26. Y. C. Li, Z. H. Wang, X. L. Li, G. Z. Xie, D. C. Chen, Y. F. Wang, C. C . Lo, A. Lien, J. B. Peng , Y. Cao, S. J. Su, *Chem. Mater.*, 2015, **27**, 1100.
27. S. J. Kim, J. Leroy, C. Zuniga, Y. D. Zhang, L. Y. Zhu, J. S. Sears, S. Barlow, J. L. Bredas, S. R. Marder, B. Kippelen, *Org. Electron.*, 2011, **12**, 1314.
28. H. Sasabe, Y. Seino, M. Kimura, J. Kido, *Chem. Mater.*, 2012, **24**, 1404.
29. H. Sasabe, N. Toyota, H. Nakanishi, T. Ishizaka, Y. J. Pu, J. Kido, *Adv. Mater.*, 2012, **24**, 3212.
30. H. F. Wang, L. L. Jiang, T. Chen, Y. M. Li, *Eur. J. Org. Chem.*, 2010, **2010**, 2324.
31. M. J. Frisch, G. W. Trucks, H. B. Schlegel, G. E. Scuseria, M. A. Robb, J. R. Cheeseman, J. A. Jr. Montgomery, T. Vreven, K. N. Kudin, J. C. Burant, J. M. Millam, S. S. Iyengar, J. Tomasi, V. Barone, B. Mennucci, M. Cossi, G.Scalmani, N. Rega, G. A. Petersson, H. Nakatsuji, M. Hada, M. Ehara, K. Toyota, R.Fukuda, J. Hasegawa, M. Ishida, T. Nakajima, Y. Honda, O. Kitao, H. Nakai, M. Klene, X. Li, J. E. Knox, H. P. Hratchian, J. B. Cross, V. Bakken, C. Adamo, J. Jaramillo, R. Gomperts, R. E. Stratmann, O. Yazyev, A. J. Austin, R. Cammi, C. Pomelli, J. W. Ochterski, P. Y. Ayala, K. Morokuma, G. A. Voth, P. Salvador, J. J. Dannenberg, V. G. Zakrzewski, S. Dapprich, A. D. Daniels, M. C. Strain, O. Farkas, D. K. Malick, A. D. Rabuck, K. Raghavachari, J. B. Foresman, J. V. Ortiz, Q. Cui, A. G. Baboul, S. Clifford, J. Cioslowski, B. B. Stefanov, G. Liu, A. Liashenko, P. Piskorz, I. Komaromi, R. L. Martin, D. J. Fox, T. Keith, M. A. Al-Laham, C. Y. Peng, A. Nanayakkara, M. Challacombe, P. M. W. Gill, B. Johnson, W. Chen, M. W. Wong, C. Gonzalez, J. A. Pople, Gaussian 09, Revision B_01, Gaussian, Inc., Wallingford, CT, 2010.
32. H. Ye, D. C. Chen, M. Liu, S. J. Su, Y. F. Wang, C. C. Lo, A. Lien, J. Kido, *Adv. Funct. Mater.*, 2014, **24**, 3268.
33.Y. Seino, H. Sasabe, Y. J. Pu, J. Kido, Adv. Mater., 2014, 26, 1612.
34. C. W. Lee, J. Y. Lee, Adv. Mater., 2013, 25, 5450.
35. H. Shin, S. Lee, K. H. Kim, C. K. Moon, S. J. Yoo, J. H. Lee , J. J. Kim, Adv. Mater., 2014, 26, 4730
36. J. H. Lee, S. H. Cheng, S. J. Yoo, H. Shin, J. H. Chang, C. I. Wu, K. T. Wong , J. J. Kim, Adv Funct Mater, 2015, 25, 361.

Table of Contents Graphic

Title: 9,9-Diphenyl-thioxanthene Derivatives as Host Materials for Highly Efficient Blue Phosphorescent Organic Light-Emitting Diodes

Authors: Kunkun Liu, Xiang-Long Li, Ming Liu, Dongcheng Chen, Xinyi Cai, Yuan-Chun Wu, Chang-Cheng Lo, A. Lien, Yong Cao, and Shi-Jian Su

A series of 9,9-diphenyl-*9H*-thioxanthene derivatives are reported as host materials in blue phosphorescent OLEDs, giving maximum power efficiency of 69.7 lm W^{-1} and external quantum efficiency of 29.0%.